Stroke Shifts Brain Dynamics Toward Criticality: Evidence from Intrinsic Neural Timescales

Kaichao Wu[1], Beth Jelfs[2], Qiang Fang[3] and Leonardo L. Gollo[1,4]

Abstract

Stroke induces widespread disruptions to brain function, extending beyond focal lesions to alter the multiscale temporal dynamics that govern neural processing. These dynamics—operating across milliseconds to months—form a hierarchical architecture essential for communication, integration, and adaptive plasticity. While stroke is known to impair local neural activity, its effects on this temporal hierarchy and their consequences for functional recovery remain poorly understood.

We conducted a comprehensive investigation of *intrinsic neural timescales* (INT) in 15 ischemic stroke patients using longitudinal fMRI at five-time points over six months, comparing them to age-matched healthy controls. INT quantifies how long neural populations retain information, providing a quantitative measure of fundamental processing dynamics. To further elucidate the mechanistic basis of stroke-induced changes, we performed computational modelling of parsimonious excitable neuronal network dynamics, offering insights into alterations in brain activity from a dynamical systems perspective.

Our analyses revealed some key findings: Stroke patients exhibited significantly prolonged INT across multiple cortical regions, indicating slowed temporal dynamics that persisted throughout recovery. The typical hierarchical organization of INT, where sensory areas have shorter timescales than higher-order association areas, was disrupted, particularly in the early post-stroke period. Recovery trajectories diverged at two months post-stroke: patients with poor outcomes maintained abnormally long INT in cognitive control networks (dorsal attention, language, and salience systems), whereas those with better recovery showed progressive normalization toward healthy INT patterns, restoring the brain's dynamic balance across multiple timescales. Stroke-induced INT prolongation can be modelled as a critical slowing down driven by a shift in the distance to criticality caused by increased neuronal excitability. Within the framework of criticality, where neural systems operate near the boundary between order and disorder to optimize information processing, stroke-induced changes in neural excitability appear to push brain dynamics toward the critical regime and potentially into a supercritical state. This shift, characterized by excessive temporal persistence and reduced flexibility, may underlie both the observed INT prolongation and its association with poor recovery outcomes.

Our findings highlight the importance of temporal dynamics in stroke recovery and suggest that INT may serve as a biomarker for predicting long-term functional outcomes. This perspective provides a novel way to conceptualize stroke-induced changes in brain dynamics, framing them within the broader context of brain self-organization and adaptive processes. By integrating these insights with neurorehabilitation strategies, such as non-invasive brain stimulation, INT could inform targeted interventions to restore neural excitability and intrinsic timescales, thereby improving recovery trajectories.

Author affiliations:

1 Brain Networks and Modelling Laboratory, The Turner Institute for Brain and Mental Health, School of Psychological Sciences, and Monash Biomedical Imaging, Monash University, Victoria 3168, Australia

2 Department of Electronic, Electrical, and Systems Engineering, University of Birmingham, Birmingham, UK.

3 Department of Biomedical Engineering, College of Engineering, Shantou University, China.

4. Institute for Cross-Disciplinary Physics and Complex Systems, IFISC (UIB-CSIC), Palma de Mallorca, Campus University de les Illes Baleares, Spain.

Correspondence to: Leonardo L. Gollo

Full address: Institute for Cross-Disciplinary Physics and Complex Systems, IFISC (UIB-CSIC), Palma de Mallorca, Campus University de les Illes Baleares, Spain.

E-mail: leonardo@ifisc.uib-csic.es

Running title: Intrinsic Neural Timescales in Stroke

Keywords: Lesion; Network disease; Dynamic system.

Introduction

The human brain operates through complex dynamics that enable flexible cognition, efficient information processing, and adaptive responses to the environment.[1-5] These dynamics emerge from interactions between neural populations and are crucial for maintaining a balance between stability and flexibility in brain function.[6] As a fundamental property of the dynamics of brain regions, intrinsic neural timescales (INT) reflect the temporal window over which neural activity is integrated.[2,3,7,8] Alterations in INT have been observed across various conditions, including temporal lobe epilepsy[9,10] Alzheimer's disease,[11] and Parkinson's disease,[12] highlighting its potential as a biomarker for disrupted neural dynamics and functional impairments. INT provides valuable insights into how neural architecture shapes functional behaviour and information processing,[8,13] and represents a critical dynamical feature linking brain structure and function. Altered INT are often related[14] or caused by alterations in gray matter volume,[15] reflecting structural and functional changes in the brain, thereby serving as a bridge between anatomical alterations and dynamic neural processes.

Despite these recent advances in our understanding of INT in different conditions, their role in stroke remains unexplored. As stroke typically causes substantial structural damage to the

brain, INT can be a relevant tool to reveal critical changes in brain dynamics. Stroke can result in localized lesions and disruptions to white matter integrity, leading to widespread functional impairments, including deficits in motor control, cognitive processes, and sensory integration.[16-18] While significant progress has been made in understanding post-stroke atypical temporal dynamics in neural activity through studies of network reorganization,[19-21] functional connectivity,[22-24] and network efficiency,[25] the specific impact of stroke lesions on INT and their role in brain function and recovery remain unclear.

Furthermore, INT is derived from the autocorrelation function (ACF) of a neural signal and is measured by its decay properties.[3,15,26,27] A slow decay of ACF, following a power-law function, occurs at a critical point and is known in the literature as critical slowing down.[6,28-31] In practical terms, this means that INT is maximized at a critical point,[15] and various computational properties are also optimized around the critical state[6,28]. This concept of criticality provides a powerful framework for linking INT to distinct dynamical states[15]: subcritical, critical, and supercritical. In the subcritical and supercritical states, INT is short due to rapid (exponential) signal decay; at criticality, they persist longer, following a slow power-law decay. Throughout this framework, criticality has been applied to various brain states,[32] including anesthesia,[33,34] epilepsy,[35,36] neurodegeneration,[37] cognition,[38,39] psychiatry,[40] and sleep medicine.[41] However, its relevance to stroke remains unexplored, presenting an opportunity to investigate how stroke lesions disrupt neural criticality and influence functional recovery. By examining INT through the lens of criticality, deeper insights into the temporal reorganization of brain dynamics after stroke and its potential role in shaping recovery trajectories can be obtained.

This longitudinal study examines how stroke disrupts the brain's multiscale temporal organization by investigating alterations in INT and their hierarchical arrangement across functional networks. Grounded in the criticality framework, we combine longitudinal fMRI with biologically inspired, parsimonious neuronal network modelling to characterize post-stroke temporal reorganization. Empirically, we track INT trajectories during recovery; computationally, we simulate how changes in neuronal excitability reshape brain network dynamics. We test a central hypothesis that stroke generates unique INT signatures that distinguish patients from healthy controls across temporal hierarchies and inform functional recovery outcomes. By bridging empirical findings with computational models of critical dynamics, this work establishes a novel understanding of post-stroke recovery that spans spatial scales, from neuronal excitability to network reconfiguration, while identifying INT as a mechanistic marker of temporal disruption and a potential clinical biomarker for prognosis.

Materials and methods

Subjects

Fifteen ischemic stroke patients (ISP) admitted to the First Affiliated Hospital of Shantou University Medical College were recruited for this study. Inclusion criteria were as follows: (i)

The first stroke or previous stroke without sequelae; (ii) The diagnosis was in line with the main points of cerebrovascular disease diagnosis approved by the fourth National Cerebrovascular Disease Academic Conference in 1995; (iii) The onset time was 2 weeks to 6 months, and Brunnstrom stage 0-3 of the affected hand; (iv) No metal implants or pacemakers in the body; (v) No previous history of epilepsy; (vi) Informed consent signed by the patient or his immediate family member. Participants were excluded if they met any of the following conditions: (i) Patients with Parkinson's disease or other neurological diseases; (ii) Patients with serious diseases of the heart, lung, and other organs; (iii) a history of mental illness, drug abuse and alcohol abuse; (iv) Patients with an unstable condition, such as blood pressure index: low-pressure <90 mmHg or high-pressure >2160 mmHg.

The fifteen patients presented with mild to severe motor function deficits (National Institutes of Health Stroke Scale, NIHSS: 7.26, 1-20). Among these patients, 6 had right-sided, and 9 had left-sided strokes, with an average age of 63.8 years (*standard deviation*: 11.68 years). The cohort consisted of 4 males and 11 females, with the first MRI scan performed on average 23.06 days post-stroke (*standard deviation*: 4.32 days). Ethical approval for the study was granted by the Medical Research Ethics Committee of the named hospital (approval number: SUMC-2021-78-K), and all participants provided written informed consent in accordance with the Declaration of Helsinki. Additionally, a control group of 15 age-matched healthy individuals with no history of stroke and a normal neurological examination (7 males, 6 females, mean age: 68.6 years, standard deviation: 6.4 years) was included for comparison. No significant differences were observed between the stroke patients and healthy controls in terms of age (p = 0.18, two-sample t-tests) or sex distribution (p = 0.17, Pearson's chi-squared test). All aspects of this study were also approved by the Monash University Human Research Ethics Committee. Demographic features of recruited stroke patients and healthy controls are listed in Table 1.

Recruited patients underwent five follow-up scans at evenly spaced intervals of 30-40 days over six months post-stroke. In practice, all recruited fifteen patients finished the follow-up plan. Recovery trajectories of patients were quantified using the Brunnstrom stage score.[42] This validated measure of upper limb motor recovery function is assessed across four dimensions. To test the association between Intrinsic neural timescales (INT) and post-stroke recovery, patients demonstrating at least 2-stage improvement by the final assessment were classified as having good recovery, while those showing improvement by one or fewer stages were classified as poor recovery.[43,44] The detailed demographic characteristics and the follow-up clinical features of stroke patients can be seen in Supplementary material Table 2. The corresponding lesion map of all stroke patients has been attached to Supplementary material Figure 1. There was no statistically significant difference in time since stroke (p = 0.59, permutation test) and size of lesion volumes (p = 0.16, permutation test) between subgroups.

fMRI Acquisition, Pre-Processing and Denoising

Resting-state fMRI data were acquired for all patients at five follow-up visits using a 3.0 T Discovery MRI scanner with an 8-channel head coil at the SUMC MRI Center. High-resolution T1-weighted anatomical images were acquired using a multi-planar rapid gradient echo sequence with the following parameters: 129 slices, repetition time (TR) = 2250 ms, echo time (TE) = 4.52 ms. Following the anatomical scan, resting-state functional MRI data were collected using a single-shot gradient-echo EPI sequence: TR = 2000 ms, TE = 30 ms, flip angle = 90°, and voxel size = 3.43 × 3.43×5.0 mm^3 (no gap). A total of 210 volumes were obtained over a 7-minute duration for each MRI scan (see Fig. 1**A**).

The fMRI data underwent preprocessing using a tailored pipeline within the CONN functional connectivity toolbox[45], integrated with the Statistical Parametric Mapping software (SPM12).[46] For fMRI from stroke patients, the bias of the hemisphere was eliminated by flipping the right hemispheric lesions to the left along the midsagittal plane(see the supplementary material Figure 1C for the left lesions of all patients). For each participant, the first 10 dummy volumes were discarded. The subsequent functional images were corrected for slice timing and head motion (no significant difference in framewise displacement detected, p = 0.99, two-sample t-tests). Outlier detection was performed using Artifact Detection Tools[45] to identify anomalous time points for each participant. These outliers were removed as covariates, and the remained function images were then normalized to the Montreal Neurological Institute (MNI) space after masking lesioned tissue.

Non-smoothed functional images were further processed through the default denoising pipeline[45], which included removing confounding effects and applying temporal band-pass filtering. Potential confounding effects in BOLD signal include noise components from (i) cerebral white matter and cerebrospinal areas, (ii) estimated motion parameters identified during the realignment step of pre-processing, (iii) outlier scans from outlier identification (i.e., scrubbing), and (iv) constant and (v) first-order linear session effects. We regressed out the five confounds, and then the residual time series was band-pass filtered in the 0.008–0.09 Hz range.[45]

Head motion control

The head motion effect was controlled by calculating the individual mean and maximum framewise displacements (FD)[47]:

$$\mathrm{FD_i} = |\Delta \mathrm{d_{ix}}| + |\Delta \mathrm{d_{iy}}| + |\Delta \mathrm{d_{iz}}| + |\Delta \alpha_\mathrm{i}| + |\Delta \beta_\mathrm{i}| + |\Delta \gamma_\mathrm{i}| \qquad (3)$$

where $\Delta d_{ix} = d_{(i-1)x} - d_{ix}$ and similarly for other rigid body parameters $[d_{ix}, d_{iy}, d_{iz}, \alpha_i, \beta_i, \gamma_i]$. Participants with a maximum displacement exceeding 1.5 mm and a maximum rotation above 1.5 degrees were excluded. While in practice, no FD was above the threshold, and no subjects were excluded. Besides, 24 motion parameters calculated from the six original motion parameters using Volterra expansion[48] were regressed out as nuisance covariates.

Brain Parcellation

To analyse changes in network dynamics resulting from stroke lesions, we utilized a functional brain parcellation derived from CONN's group independent component analysis (ICA) of the HCP dataset (497 subjects). This parcellation includes 32 regions of interest (ROIs) spanning the entire brain, grouped into eight large-scale functional networks or systems: Default mode network (DMN); Sensorimotor network (SMN); Visual network (VIS); Dorsal attention network (DAN); Salience network (SAN); Frontoparietal network (FPN); Language network (LN); Cerebellar network(CE) (see Supplementary material Table 2 for the details of eight large-scale functional network and 32 ROI as well as their peak coordinates). ICA spatial maps were applied to each participant's fMRI BOLD data to extract a representative timeseries for each ROI (see Fig. 1**B** for parcellation map).

Estimation of Intrinsic Neural Timescales

We estimated intrinsic timescale values for all regional BOLD timeseries. This involves first computing the autocorrelation function (ACF) for each timeseries:

$$ACF_k = \frac{\sum_{t=k+1}^{T}(y_t - \bar{y})(y_{t-k} - \bar{y})}{\sum_{t=1}^{T}(y_t - \bar{y})^2} \tag{1}$$

where y denotes the preprocessed regional BOLD timeseries, $\bar{y}$ is the mean value across time points. t is the length of time bins, which is the time of repetition (TR = 2000 ms) of the MRI scan, and T is the number of time points (200 in the experiment).

Next, the intrinsic timescale was calculated as the area under the curve of the autocorrelation function from one to the time lag that the correlation reaches zero (see Fig. 1**C** for illustration.):

$$INT = TR \cdot \sum_{k=1}^{n_{lag}-1} ACF_k, ACF_{n_{lag}} < 0 \quad (2)$$

This process was applied to all regional BOLD timeseries of patients and healthy controls, resulting in an intrinsic timescale map for the entire brain network for each participant.

Intrinsic Neural Timescales and Distance to Criticality

To interpret INT abnormalities in stroke, we employed a parsimonious neuronal network modelling approach to investigate how intrinsic timescales vary with neural excitability. In particular, a random network of $N = 100{,}000$ excitable spiking neurons and mean average degree $K = 10$ were utilized to initialize brain neuronal networks. The neuronal network dynamics were then modelled using the Kinouchi-Copelli model.[49] Each neuron is a cyclic cellular automaton that follows a discrete-time process defined on the state space (quiescent, spike and refractory). When at a quiescent state, neurons can spike by (i) an external drive modelled as a Poisson process with probability with the rate $r = 10^{-5}$, which activates neurons with probability $h = 1 - e^{-r \cdot \delta_t}$ where $\delta_t = 1$ ms is the time step, or by (ii)

receiving input propagation from a spiking connected neuron with probability λ. The spiking neuron will enter a refractory state at the next time step and then enter the quiescent state after a period of 8 ms. The neuronal network activity is defined as the instantaneous density of active neurons as functions of time.

The branching ratio ($\sigma = K \cdot \lambda$) of the neuronal networks represent the average number of spikes generated by each excited neuron in the next time step. The brain is in a critical state when $\sigma = 1$, where the network activity propagates in a balanced manner, maximizing information transfer and computational efficiency.[6,50-52] In the subcritical state ($\sigma < 1$) activity decays rapidly, leading to diminished neural interactions and reduced information integration. Conversely, in the supercritical state ($\sigma > 1$) activity grows excessively. For branching processes, the branching ratio can indicate deviations from criticality, which is known as the distance to criticality (*DTC*), where $DTC = 1 - \sigma$ in subcritical states and $DTC = \sigma - 1$ in supercritical states. The INT is maximized at the critical state, and it decreases with DTC towards both sub- and supercritical states.[15]

Due to the nature of the branching ratio, changes in network degree K or the propagation probability λ will affect σ and, thus cause alterations in INT. The effects of varying K and N on the relationship between INT and *DTC* was previously explored in the context of aging.[15] Given that stroke often results in hyperexcitability[53,54,55,56] and an increased risk of seizures, here we vary λ to capture how stroke-induced changes in neural excitability and examine how stroke affects the relationship between *DTC* and INT.

Statistical Analysis

Welch's t-test was performed to investigate if there were statistically significant differences in the whole brain, global average, and network-level INT between healthy controls and patients. Repeated-measures one-way ANOVA (level of significance $p < 0.05$ false discovery rate (FDR) corrected[57]) was used to test if INT significantly differed across different time points. Two-way ANOVA was used to test if the recovery outcome and functional network have an effect on INT. In the case of significant ANOVA results, post hoc t-tests were performed.

Results

Demographic and clinical characteristics

There were no significant differences in age, sex category and mean framewise displacement between stroke patients and healthy controls (Table 1). Patients were first scanned on an average of 23.06 days (standard deviation: 4.32 days) after stroke onset. Recruited patients underwent five follow-up scans at evenly spaced intervals of 30-40 days over six months post-stroke. Recovery trajectories of patients were quantified using the Brunnstrom stage score[42]. We use 2-stage improvements at the final assessment as a cutoff to distinguish the

good (n = 6) and poor (n = 9) recovery subgroups[43,44]. There are no significant differences in age or sex categories between the two groups, while the lesion volume is higher in the poor outcome group (3.93±2.24 cm^3) than in the good outcome group (19.43±19.54 cm^3). The details of recovery outcome assessment at each follow-up for both groups can be seen in Supplementary material Table 2.

Abnormal INT Following Stroke

One month after the stroke, stroke patients showed significantly longer intrinsic neural timescales compared to healthy controls, both globally (Fig. 1**D**) and within each specific functional network (Fig. 1**E**). The global average INT was notably higher in stroke patients (t = 8.23, p < 0.0001, Welch's t-test), highlighting widespread alterations in the temporal dynamics of brain activity. When examining specific functional networks, stroke patients showed significant increases in INT across all networks see the statistic and p values in Table 2.

Reconfigured Hierarchical INT in Post-stroke Patients

In addition to the global and network-specific abnormalities in INT, stroke patients exhibited a significant disruption in the hierarchical organization of INT. In healthy controls (Fig. 1**F**), we found INT are well-ordered and exhibit a stable hierarchy across functional networks, with the CE network having the shortest INT (*Mean* ± *Std*: 1.422± 0.257) while SMN has the longest INT (*Mean* ± *Std* :1.626 ± 0.389). These results align with previous findings on the hierarchical organization of INT, where unimodal regions, such as the cerebellar network, exhibit shorter timescales, while transmodal regions, including the frontoparietal network (FPN) and default mode network (DMN), demonstrate longer timescales, reflecting the brain's capacity to maintain network specialization and efficient information processing.[4,5,7]

However, this hierarchical organization was severely disrupted in stroke patients at 1 month post-stroke (Spearman's *rho* = -0.90, p < 0.0001), as shown in Fig. 1**F**. Strikingly, the cerebellar network (CE) showed the largest difference (*Mean* ± *Std*: 8.178 ± 5.901), as it showed the shortest INT in the control group but the longest INT in stroke patients. Furthermore, the DMN, which had long INT for controls, exhibited the shortest INT in stroke patients (*Mean* ± *Std*: 6.068 ± 2.875). However, despite this relative decrease within the stroke group, the INT of the DMN remained longer than that of the controls.

The Development of INT within Six Months After Stroke

The global average INT was compared between healthy controls and stroke patients across different time points post-stroke to examine the development within a six-month period post-stroke (Fig. 2**A**). Repeated-measures one-way ANOVA analysis revealed significant differences in INT (F = 13.05, p < 0.0001, FDR corrected). The post-hoc t-test indicates that the prolonged INT observed in stroke patients persists for at least five months after the stroke attack ($t_{CTR\text{-}PAT1}$ = 8.22, p<0.0001; $t_{CTR\text{-}PAT2}$ = 10.80, p < 0.0001; $t_{CTR\text{-}PAT3}$ = 5.94, p < 0.0001;

$t_{\text{CTR-PAT4}}$ = 7.61, p < 0.0001; $t_{CTR\text{-}PAT5}$ = 5.80, p < 0.0001.). This enduring elevation in INT suggests a long-lasting disruption in the brain's temporal dynamics following a stroke, as depicted in the global INT comparisons. A whole-brain map of the prolonged INT in stroke patients at different time points further highlights the widespread nature of these changes (the example of PAT1 can be seen in Fig. 2**B**.

INT as A Prognostic Biomarker for Recovery

To further explore recovery dynamics, patients were categorized into two groups according to motor function outcomes nearly six months later: the good and the poor recovery group. At 2 months post-stroke (PAT2), a significant difference in INT emerged between the two groups (Fig. 2**C**), with the poor recovery group exhibiting significantly longer INT than the good recovery group ($t_{poor\text{-}good}$ = 2.30, p = 0.03). This finding suggests that differences in INT at 2 months post-stroke may serve as an early predictor of recovery outcomes six months later, highlighting the potential utility of INT as a prognostic biomarker.

A two-way ANOVA was then used at PAT2 to test whether the recovery outcomes (good vs. poor) and the functional networks (DMN, SMN, DAN, etc.) have an effect on INT. We found a statistically significant difference in INT by both outcomes (F = 11.99, p < 0.001, FDR corrected) and by various function networks (F = 3.83, p < 0.001, FDR corrected), though the interaction between these terms was not significant.

Post-hoc t-test analysis revealed network-specific significant differences in INT between the pairwise recovery groups (Fig. 2D). Patients with good recovery outcomes exhibited notably shorter INT compared to those with poor recovery outcomes in the salience network (SAN; $t_{good\text{-}poor}$ = -3.10, p = 0.016), dorsal attention network (DAN; $t_{good\text{-}poor}$ =-5.96, p = 0.006) and language network (LN; $t_{good\text{-}poor}$ = -4.31, p = 0.031). These findings indicate that lower INT within specific functional networks is associated with better recovery trajectories, further emphasizing the role of INT as a network-level biomarker for predicting post-stroke recovery outcomes.

Distance to Criticality Explain the Abnormal INT in Stroke

Finally, we interpret the abnormal INT in stroke within the criticality framework. By fixing the network mean degree (K) and varying the propagation probability (λ), we control the branching ratio (σ), a key metric that governs neural activity spread and serves as an indicator of criticality. The activity is defined as the instantaneous density of active neurons as functions of time. The examples of neuronal network activities simulated with various σ = [0.08, 0.1, 0.12] with fixed $K = 10$, which represent the subcritical, critical, and supercritical, can be seen in Supplementary material Figure 2A. The corresponding autocorrelation curves, which are used to compute the INT, have been in Supplementary material Figure 2B. As shown in Fig. 3, INT and overall network activity (inset) are directly shaped by σ. Notably, intrinsic timescales increase sharply as the network approaches the critical point ($\sigma = 1$), a hallmark of critical slowing down (see Supplementary material Figure 2C for the single trial relationship between the INT and criticality). When linked to

the prolonged INT observed in stroke patients, these results suggest that stroke increases neural excitability (reflected by λ), shifting brain dynamics closer to criticality and reducing the distance to criticality (*DTC*). This shift renders post-stroke neural networks more susceptible to prolonged activity fluctuations, potentially pushing the system into a supercritical state. Such a transition may drive maladaptive neuroplasticity, contributing to dysfunctional network reorganization and impairing recovery trajectories in stroke patients.

Data availability

The raw MRI scan of patients and control will be available upon request after signing the anonymous data protocol. The source data for the main figures presented in the paper are attached. The customized Python codes for data and statistics analysis and network modelling are available in the GitHub repository https://github.com/xiaohajiayouo/Stroke-Alters-Intrinsic-Neural-Timescales-and-Their-Hierarchical-Organization.

Discussion

This study investigates the impact of stroke on intrinsic neural timescales and their dynamics during recovery by analysing functional neuroimaging data from ischemic stroke patients over a six-month post-stroke period. Our findings reveal that stroke induces persistent disruptions in INT, both globally and within specific functional networks, reflecting altered temporal dynamics and hierarchical organization. Notably, differences in INT between patients with good and poor recovery outcomes emerge at two months post-stroke, highlighting the potential of INT as a predictor of long-term recovery. The observation of significantly shorter INT in patients with good outcomes further suggests that post-stroke recovery may involve the normalization of INT. These insights advance our understanding of post-stroke brain dynamics and underscore the potential of INT as a biomarker for recovery trajectories.

Changes in INT have been observed across the lifespan, with longer INT in young adults compared to elderly individuals.[15] Atypical INT patterns have also been widely documented in various brain disorders, including shorter INT in sensory regions in autism[14], mixed patterns in schizophrenia (shorter in parietal and occipital regions[58] but longer in self-referential processes,[59] and shorter INT in Alzheimer's disease[11] and temporal lobe epilepsy.[9,10] Additionally, significant differences in INT have been reported in Parkinson's disease, with shorter INT in late-stage and longer INT in early-stage patients.[12]

Building on this foundation, this study investigates how stroke affects INT and its dynamics during recovery. Our results reveal that stroke patients exhibit significantly elevated INT compared to healthy controls, with this increase persisting throughout the five-month follow-up period. This prolonged elevation aligns with findings from electroencephalography (EEG) and magnetoencephalography (MEG) studies, which demonstrate that stroke causes widespread slowing of neural activity.[60,61] The persistent increase in INT suggests enduring

disruptions in the temporal integration of neural activity,[7,8] likely reflecting widespread dysfunction in brain network dynamics.[19-21]

The consistent elevation of INT across key functional networks—including the default mode network (DMN), salience network (SAN), and frontoparietal network (FPN)—indicates a global impact of stroke. This disruption may impair functional specialization[62,63] and network efficiency,[25] contributing to the cognitive and motor deficits commonly observed in stroke patients.[62,64]

In addition to elevated INT, our study revealed a significant disruption in the hierarchical organization of INT in stroke patients. The hierarchy INT is consistently observed across both small,[13,65,66] and large-scale fMRI datasets.[4,5] Unimodal regions, such as sensory and motor networks, typically exhibit shorter INT, whereas transmodal regions, including higher-order networks like the central-executive network (CEN), dorsal attention network (DAN), and default-mode network (DMN), tend to display longer INT.[5,7,65,67,68] Our finding of INT in healthy individuals supports and extends the hierarchical organization of INT, demonstrating that temporal dynamics across networks are balanced and optimized for efficient information processing and integration.[7,13] However, this organization was severely disrupted following a stroke, as indicated by a strong negative correlation in the INT hierarchy. The cerebellum network, whose function is associated with motor coordination and learning, including balance and posture, as well as other cognitive functions,[69] was affected the most. This likely reflects the importance of the cerebellum network in the reconfiguration of brain dynamics involving motor but also other cognitive functions. In a similar vein, during this reconfiguration, the default mode network (DMN), which typically exhibits long INT[13] and stable dynamics,[70,71] also demonstrated significant changes in its dynamics, showing the shortest INT and the least stability among functional networks in stroke patients.[72]

A key finding of this study is the divergence in INT trajectories based on recovery outcomes.[16,44,64,72] At two months post-stroke, patients with poor recovery exhibited significantly longer INT than those with good recovery. This suggests that early-stage INT measurements could serve as a predictive marker for long-term outcomes. In addition, this finding also led to the hypothesis that good recovery could be associated with a normalization of the altered INT, i.e., a network reduction in the magnitude of INT (for example salient network and dorsal attention network), whereas poor recovery could be associated with an inability to promptly recover the abnormal INT to normal levels. These findings align with the potential of the temporal profile of the responses to transcranial magnetic stimulation observed in EEG signals following stroke.[73]

The relationship between stroke and intrinsic neural timescales can be understood through the framework of criticality,[6 28,32,50,74] which posits that the brain operates near a transition point between ordered and disordered states to benefit from its optimal computational properties. Shifts in the distance to criticality have been applied to various clinical contexts, including depression,[30,75] schizophrenia,[76,77] epilepsy,[78,79] insomnia,[79] Alzheimer's disease,[80] Parkinson's disease,[81] and also states like aging,[15,82-85] anesthesia,[86] meditation,[87] cognitive tasks,[88] sleep homeostasis,[89] and sustained wakefulness.[90] Intrinsic neural timescales, reflecting long-range temporal correlations, serve as a proxy for the brain's proximity to

criticality. Stroke disrupts this balance through mechanisms such as excitotoxicity, inflammation, and maladaptive plasticity, often resulting in hyperexcitability and an increased risk of seizures[91-93]. Post-stroke brains exhibit prolonged intrinsic timescales compared to healthy controls, indicating a shift toward criticality (see Fig. 3) and potentially into a supercritical state, where pathological dynamics—such as aberrant synchronization and excessive firing—can emerge. This shift aligns with the criticality model, in which intrinsic timescales—derived from the autocorrelation function, commonly used to measure the distance to criticality[94]—peak at criticality and decay in both subcritical and supercritical regimes,[15] linking post-stroke changes in temporal dynamics to network instability.

Notably, INT is unevenly affected across the brain, causing alterations in the hierarchy of timescales, as some brain regions are more affected than others. This disruption in the hierarchical organization of timescales further highlights how stroke-induced changes can lead to an imbalance in the brain's functional networks. Thus, the criticality framework provides a unifying perspective on stroke-induced disruptions, translating the complexity of molecular and vascular processes into their net effect on neural excitability. However, variability in stroke location and severity complicates the clinical quantification of deviations from criticality in individual patients. Despite these challenges, criticality remains a valuable conceptual tool for understanding how stroke alters intrinsic timescales and brain network dynamics.

Our findings suggest that the prolonged INT observed in stroke patients may reflect a maladaptive shift in neural dynamics, driven by excessive network persistence and impaired information processing. The observed association between shorter INT and improved recovery highlights the potential of modulating INT as a therapeutic target for functional restoration.[8] Given the strong link between INT, neuronal excitability, and network interactions, our results indicate non-invasive brain stimulation (NIBS) techniques—such as transcranial magnetic stimulation (TMS) and transcranial electrical stimulation (TES)—as promising strategies to normalize aberrant INT.[1,8,95-100] Specifically, excitatory stimulation (e.g., anodal transcranial direct current stimulation, high-frequency TMS, intermittent theta burst stimulation, and entrainment by transcranial alternating current stimulation[101]) could be used to reduce abnormally prolonged INT, aligning with the dynamics observed in patients with better recovery outcomes.[100] By targeting influential hub regions or larger brain systems with altered INT, NIBS offers a novel therapeutic avenue to restore balanced network dynamics, enhance functional recovery, and improve post-stroke outcomes. Future research integrating real-time neurophysiological monitoring and computational modelling could further refine these interventions,[97] enabling personalized stimulation protocols tailored to individual neurophysiological profiles. This approach holds significant promise for optimizing recovery trajectories and advancing precision medicine in stroke rehabilitation.

Future Directions

This study provides valuable insights into the neural dynamics of stroke recovery and underscores important avenues for future exploration. The longitudinal design, featuring five follow-ups over six months, provides a robust framework for investigating INT in stroke

patients and could be extended to refine recovery trajectory models. The sample size (N=15) provides meaningful insights and establishes a strong foundation for future large-scale studies to further validate and expand upon these findings. Additionally, the focus of the study on fMRI data opens the possibility for integrating multimodal approaches—such as EEG or diffusion-weighted imaging—that could deepen our understanding of the temporal and structural changes associated with INT dynamics.

The identification of meaningful patterns of INT across functional networks marks a notable advancement. Future research utilizing advanced techniques, such as machine learning or personalized network analyses, holds significant potential to reveal individual-level variability and improve predictive accuracy. While this study concentrated on motor recovery, exploring the impact of INT on cognitive and sensory outcomes offers a promising direction for future research, providing new insights into post-stroke rehabilitation.

Acknowledgements

This study acknowledges the Shantou University Medical College for the help of patient recruitment and MRI scan acquisition.

Funding

This work was supported by the Australian Research Council (ARC), Future Fellowship (FT200100942), the Ramón y Cajal Fellowship (RYC2022-035106-I) from FSE/Agencia Estatal de Investigación (AEI), Spanish Ministry of Science and Innovation, and the María de Maeztu Program for units of Excellence in R&D, grant CEX2021-001164-M.

Competing interests

The authors report no competing interests.

References

1. Golesorkhi M, Gomez-Pilar J, Zilio F, et al. The brain and its time: intrinsic neural timescales are key for input processing. *Communications biology*. 2021;4(1):970.
2. Wolman A, Çatal Y, Wolff A, et al. Intrinsic neural timescales mediate the cognitive bias of self–temporal integration as key mechanism. *NeuroImage*. 2023;268:119896.
3. Murray JD, Bernacchia A, Freedman DJ, et al. A hierarchy of intrinsic timescales across primate cortex. *Nature neuroscience*. 2014;17(12):1661-1663.
4. Burt JB, Demirtaş M, Eckner WJ, et al. Hierarchy of transcriptomic specialization across human cortex captured by structural neuroimaging topography. *Nature neuroscience*. 2018;21(9):1251-1259.

5. Ito T, Hearne LJ, Cole MW. A cortical hierarchy of localized and distributed processes revealed via dissociation of task activations, connectivity changes, and intrinsic timescales. *NeuroImage*. 2020;221:117141.
6. Cocchi L, Gollo LL, Zalesky A, Breakspear M. Criticality in the brain: A synthesis of neurobiology, models and cognition. *Progress in neurobiology*. 2017;158:132-152.
7. Wolff A, Berberian N, Golesorkhi M, Gomez-Pilar J, Zilio F, Northoff G. Intrinsic neural timescales: temporal integration and segregation. *Trends in cognitive sciences*. 2022;26(2):159-173.
8. Gollo LL. Exploring atypical timescales in the brain. *Elife*. 2019;8:e45089.
9. Xie K, Royer J, Lariviere S, et al. Atypical intrinsic neural timescales in temporal lobe epilepsy. *Epilepsia*. 2023;64(4):998-1011.
10. Wang K, Zhang X, Song C, et al. Decreased intrinsic neural timescales in mesial temporal lobe epilepsy. *Frontiers in human neuroscience*. 2021;15:772365.
11. Murai SA, Mano T, Sanes JN, Watanabe T. Atypical intrinsic neural timescale in the left angular gyrus in Alzheimer's disease. *Brain communications*. 2024;6(4):fcae199.
12. Wei Y, Zhang C, Peng Y, et al. MRI assessment of intrinsic neural timescale and gray matter volume in Parkinson's disease. *Journal of Magnetic Resonance Imaging*. 2024;59(3):987-995.
13. Wu K, Gollo LL. Dendrites contribute to the gradient of intrinsic timescales encompassing cortical and subcortical brain networks. *Frontiers in Cellular Neuroscience*. 2024;18:1404605.
14. Watanabe T, Rees G, Masuda N. Atypical intrinsic neural timescale in autism. *Elife*. 2019;8:e42256.
15. Wu K, Gollo LL. Mapping and modeling age-related changes in intrinsic neural timescales. *Communications Biology*. 2025;8(1):167.
16. Carrera E, Tononi G. Diaschisis: Past, present, future. *Brain*. 2014;137(9):2408-2422.
17. Park C-h, Chang WH, Ohn SH, et al. Longitudinal changes of resting-state functional connectivity during motor recovery after stroke. *Stroke*. 2011;42(5):1357-1362.
18. Volz LJ, Rehme AK, Michely J, et al. Shaping early reorganization of neural networks promotes motor function after stroke. *Cerebral cortex*. 2016;26(6):2882-2894.
19. Wu K, Fang Q, Neville K, Jelfs B. Evaluation of module dynamics in functional brain networks after stroke. In: *inproceedings*. 2023:1-4.
20. Bonkhoff AK, others. Acute ischaemic stroke alters the brain's preference for distinct dynamic connectivity states. *Brain*. 2020;143(5):1525-1540.
21. Wu K, Jelfs B, Neville K, Mahmoud SS, He W, Fang Q. Dynamic Reconfiguration of Brain Functional Network in Stroke. *IEEE Journal of Biomedical and Health Informatics*. 2024;
22. Hu J, Du J, Xu Q, et al. Dynamic network analysis reveals altered temporal variability in brain regions after stroke: A longitudinal resting-state fMRI study. *Neural plasticity*. 2018;2018(1):9394156.
23. Chen J, Sun D, Shi Y, et al. Alterations of static functional connectivity and dynamic functional connectivity in motor execution regions after stroke. *Neuroscience letters*. 2018;686:112-121.
24. Nicolo P, Rizk S, Magnin C, Pietro MD, Schnider A, Guggisberg AG. Coherent neural oscillations predict future motor and language improvement after stroke. *Brain*. 2015;138(10):3048-3060.
25. Vecchio F, others. Cortical connectivity from EEG data in acute stroke: A study via graph theory as a potential biomarker for functional recovery. *Int J Psychophysiol*. 2019;146:133-138.

26. Cavanagh SE, Hunt LT, Kennerley SW. A diversity of intrinsic timescales underlie neural computations. *Frontiers in Neural Circuits*. 2020;14:615626.
27. Wengler K, Goldberg AT, Chahine G, Horga G. Distinct hierarchical alterations of intrinsic neural timescales account for different manifestations of psychosis. *elife*. 2020;9:e56151.
28. Munoz MA. Colloquium: Criticality and dynamical scaling in living systems. *Reviews of Modern Physics*. 2018;90(3):031001.
29. Scheffer M, Bascompte J, Brock WA, et al. Early-warning signals for critical transitions. *Nature*. 2009;461(7260):53-59.
30. van de Leemput IA, Wichers M, Cramer AO, et al. Critical slowing down as early warning for the onset and termination of depression. *Proceedings of the National Academy of Sciences*. 2014;111(1):87-92.
31. Morr A, Boers N. Detection of approaching critical transitions in natural systems driven by red noise. *Physical Review X*. 2024;14(2):021037.
32. Zimmern V. Why brain criticality is clinically relevant: a scoping review. *Frontiers in neural circuits*. 2020;14:54.
33. Thiery T, Lajnef T, Combrisson E, et al. Long-range temporal correlations in the brain distinguish conscious wakefulness from induced unconsciousness. *Neuroimage*. 2018;179:30-39.
34. Krzemiński D, Kamiński M, Marchewka A, Bola M. Breakdown of long-range temporal correlations in brain oscillations during general anesthesia. *Neuroimage*. 2017;159:146-158.
35. Witton C, Sergeyev SV, Turitsyna EG, et al. Rogue bioelectrical waves in the brain: the Hurst exponent as a potential measure for presurgical mapping in epilepsy. *Journal of Neural Engineering*. 2019;16(5):056019.
36. Arviv O, Medvedovsky M, Sheintuch L, Goldstein A, Shriki O. Deviations from critical dynamics in interictal epileptiform activity. *Journal of Neuroscience*. 2016;36(48):12276-12292.
37. West T, Farmer S, Berthouze L, et al. The parkinsonian subthalamic network: measures of power, linear, and non-linear synchronization and their relationship to L-DOPA treatment and OFF state motor severity. *Frontiers in human neuroscience*. 2016;10:517.
38. Ouyang G, Hildebrandt A, Schmitz F, Herrmann CS. Decomposing alpha and 1/f brain activities reveals their differential associations with cognitive processing speed. *NeuroImage*. 2020;205:116304.
39. Ezaki T, Fonseca dos Reis E, Watanabe T, Sakaki M, Masuda N. Closer to critical resting-state neural dynamics in individuals with higher fluid intelligence. *Communications biology*. 2020;3(1):52.
40. Moran JK, Michail G, Heinz A, Keil J, Senkowski D. Long-range temporal correlations in resting state beta oscillations are reduced in schizophrenia. *Frontiers in psychiatry*. 2019;10:517.
41. Bocaccio H, Pallavicini C, Castro MN, et al. The avalanche-like behaviour of large-scale haemodynamic activity from wakefulness to deep sleep. *Journal of the Royal Society Interface*. 2019;16(158):20190262.
42. Shah SK, Harasymiw SJ, Stahl PL. Stroke rehabilitation: outcome based on Brunnstrom recovery stages. *The Occupational Therapy Journal of Research*. 1986;6(6):365-376.
43. Naghdi S, Ansari NN, Mansouri K, Hasson S. A neurophysiological and clinical study of Brunnstrom recovery stages in the upper limb following stroke. *Brain injury*. 2010;24(11):1372-1378.

44. Wu K, Jelfs B, Neville K, Fang Q. Dynamic Brain Behaviours in Stroke: A Longitudinal Investigation Based on fMRI Analysis. *arXiv preprint arXiv:240108607*. 2023;
45. Whitfield-Gabrieli S, Nieto-Castanon A. CONN: a functional connectivity toolbox for correlated and anticorrelated brain networks. *Brain Connect*. 2012;2(3):125-141.
46. Penny WD, Friston KJ, Ashburner JT, Kiebel SJ, Nichols TE. *Statistical parametric mapping: the analysis of functional brain images*. Elsevier; 2011.
47. Power JD, Barnes KA, Snyder AZ, Schlaggar BL, Petersen SE. Spurious but systematic correlations in functional connectivity MRI networks arise from subject motion. *Neuroimage*. 2012;59(3):2142-2154.
48. Palm G, Poggio T. The Volterra representation and the Wiener expansion: validity and pitfalls. *SIAM Journal on Applied Mathematics*. 1977;33(2):195-216.
49. Kinouchi O, Copelli M. Optimal dynamical range of excitable networks at criticality. *Nature physics*. 2006;2(5):348-351.
50. Heiney K, Huse Ramstad O, Fiskum V, et al. Criticality, connectivity, and neural disorder: a multifaceted approach to neural computation. *Frontiers in computational neuroscience*. 2021;15:611183.
51. Larremore DB, Shew WL, Ott E, Sorrentino F, Restrepo JG. Inhibition causes ceaseless dynamics in networks of excitable nodes. *Physical review letters*. 2014;112(13):138103.
52. Larremore DB, Shew WL, Restrepo JG. Predicting criticality and dynamic range in complex networks: effects of topology. *Physical review letters*. 2011;106(5):058101.
53. Stampanoni Bassi M, Iezzi E, Gilio L, Centonze D, Buttari F. Synaptic plasticity shapes brain connectivity: implications for network topology. *International journal of molecular sciences*. 2019;20(24):6193.
54. Carmichael ST. Brain excitability in stroke: the yin and yang of stroke progression. *Archives of neurology*. 2012;69(2):161-167.
55. Bütefisch CM, Netz J, Wessling M, Seitz RJ, Hömberg V. Remote changes in cortical excitability after stroke. *Brain*. 2003;126(2):470-481.
56. Cirillo C, Brihmat N, Castel-Lacanal E, et al. Post-stroke remodeling processes in animal models and humans. *Journal of Cerebral Blood Flow & Metabolism*. 2020;40(1):3-22.
57. Benjamini Y, Hochberg Y. Controlling the false discovery rate: a practical and powerful approach to multiple testing. *Journal of the Royal statistical society: series B (Methodological)*. 1995;57(1):289-300.
58. Usctescu LC, Said-Yrekli S, Kronbichler L, et al. Reduced intrinsic neural timescales in schizophrenia along posterior parietal and occipital areas. *NPJ schizophrenia*. 2021;7(1):55.
59. Northoff G, Sandsten KE, Nordgaard J, Kjaer TW, Parnas J. The self and its prolonged intrinsic neural timescale in schizophrenia. *Schizophrenia bulletin*. 2021;47(1):170-179.
60. Cohn R, RAINES GEORGEN, MULDER DONALDW, NEUMANN METAA. Cerebral vascular lesions: electroencephalographic and neuropathologic correlations. *Archives of Neurology \& Psychiatry*. 1948;60(2):165-181.
61. Johnston PR, Griffiths JD, Rokos L, McIntosh AR, Meltzer JA. Secondary thalamic dysfunction underlies abnormal large-scale neural dynamics in chronic stroke. *Proceedings of the National Academy of Sciences*. 2024;121(46):e2409345121.
62. Cassidy JM, Mark JI, Cramer SC. Functional connectivity drives stroke recovery: shifting the paradigm from correlation to causation. *Brain*. 2022;145(4):1211-1228.
63. Ismail UN, Yahya N, Manan HA. Investigating functional connectivity related to stroke recovery: A systematic review. *Brain Research*. 2024:149023.

64. Wu K, Jelfs B, Neville K, Cai A, Fang Q. fMRI-based static and dynamic functional connectivity analysis for post-stroke motor dysfunction patient: a review. *IEEE Access*. 2024;
65. Raut RV, Mitra A, Marek S, et al. Organization of propagated intrinsic brain activity in individual humans. *Cerebral Cortex*. 2020;30(3):1716-1734.
66. Wasmuht DF, Spaak E, Buschman TJ, Miller EK, Stokes MG. Intrinsic neuronal dynamics predict distinct functional roles during working memory. *Nature communications*. 2018;9(1):3499.
67. Huntenburg JM, Bazin P-L, Margulies DS. Large-scale gradients in human cortical organization. *Trends in cognitive sciences*. 2018;22(1):21-31.
68. Demirtaş M, Burt JB, Helmer M, et al. Hierarchical heterogeneity across human cortex shapes large-scale neural dynamics. *Neuron*. 2019;101(6):1181-1194. e13.
69. Strick PL, Dum RP, Fiez JA. Cerebellum and nonmotor function. *Annual review of neuroscience*. 2009;32(1):413-434.
70. Gollo LL, Zalesky A, Hutchison RM, Van Den Heuvel M, Breakspear M. Dwelling quietly in the rich club: brain network determinants of slow cortical fluctuations. *Philosophical Transactions of the Royal Society B: Biological Sciences*. 2015;370(1668):20140165.
71. Ponce-Alvarez A. Network mechanisms underlying the regional diversity of variance and time scales of the brain's spontaneous activity fluctuations. *Journal of Neuroscience*. 2025;
72. Bonkhoff AK, others. Abnormal dynamic functional connectivity is linked to recovery after acute ischemic stroke. *Hum Brain Mapp*. 2021;42(7):2278-2291.
73. Tscherpel C, Dern S, Hensel L, Ziemann U, Fink GR, Grefkes C. Brain responsivity provides an individual readout for motor recovery after stroke. *Brain*. 2020;143(6):1873-1888.
74. O'Byrne J, Jerbi K. How critical is brain criticality? *Trends in Neurosciences*. 2022;45(11):820-837.
75. Linkenkaer-Hansen K, Monto S, Rytsl H, Suominen K, Isomets E, Khknen S. Breakdown of long-range temporal correlations in theta oscillations in patients with major depressive disorder. *Journal of Neuroscience*. 2005;25(44):10131-10137.
76. Rolls ET, Loh M, Deco G, Winterer G. Computational models of schizophrenia and dopamine modulation in the prefrontal cortex. *Nature Reviews Neuroscience*. 2008;9(9):696-709.
77. Nikulin VV, Jnsson EG, Brismar T. Attenuation of long-range temporal correlations in the amplitude dynamics of alpha and beta neuronal oscillations in patients with schizophrenia. *Neuroimage*. 2012;61(1):162-169.
78. Yan J, Wang Y, Ouyang G, et al. Analysis of electrocorticogram in epilepsy patients in terms of criticality. *Nonlinear Dynamics*. 2016;83:1909-1917.
79. Minadakis G, Ventouras E, Gatzonis SD, et al. Dynamics of regional brain activity in epilepsy: a cross-disciplinary study on both intracranial and scalp-recorded epileptic seizures. *Journal of Neural Engineering*. 2014;11(2):026012.
80. Jiang L, Sui D, Qiao K, Dong H-M, Chen L, Han Y. Impaired functional criticality of human brain during Alzheimer's disease progression. *Scientific reports*. 2018;8(1):1324.
81. Hausdorff JM. Gait dynamics in Parkinson's disease: common and distinct behavior among stride length, gait variability, and fractal-like scaling. *Chaos: An Interdisciplinary Journal of Nonlinear Science*. 2009;19(2)
82. Berthouze L, James LM, Farmer SF. Human EEG shows long-range temporal correlations of oscillation amplitude in Theta, Alpha and Beta bands across a wide age range. *Clinical Neurophysiology*. 2010;121(8):1187-1197.

83. Smit DJA, de Geus EJC, van de Nieuwenhuijzen ME, et al. Scale-free modulation of resting-state neuronal oscillations reflects prolonged brain maturation in humans. *Journal of Neuroscience*. 2011;31(37):13128-13136.
84. Mareš J, Vyšata O, Procházka A, Vališ M. Age-dependent complex noise fluctuations in the brain. *Physiological Measurement*. sep 2013;34(10):1269.
85. Fosque LJ, Alipour A, Zare M, Williams-Garca RV, Beggs JM, Ortiz G. Quasicriticality explains variability of human neural dynamics across life span. *Frontiers in Computational Neuroscience*. 2022;16:1037550.
86. Alonso LM, Proekt A, Schwartz TH, Pryor KO, Cecchi GA, Magnasco MO. Dynamical criticality during induction of anesthesia in human ECoG recordings. *Frontiers in neural circuits*. 2014;8:20.
87. Irrmischer M, Houtman SJ, Mansvelder HD, Tremmel M, Ott U, Linkenkaer-Hansen K. Controlling the temporal structure of brain oscillations by focused attention meditation. *Human brain mapping*. 2018;39(4):1825-1838.
88. Fagerholm ED, Lorenz R, Scott G, et al. Cascades and cognitive state: focused attention incurs subcritical dynamics. *Journal of Neuroscience*. 2015;35(11):4626-4634.
89. Ribeiro TL, Copelli M, Caixeta F, et al. Spike avalanches exhibit universal dynamics across the sleep-wake cycle. *PloS one*. 2010;5(11):e14129.
90. Meisel C, Bailey K, Achermann P, Plenz D. Decline of long-range temporal correlations in the human brain during sustained wakefulness. *Scientific reports*. 2017;7(1):11825.
91. Altman K, Shavit-Stein E, Maggio N. Post stroke seizures and epilepsy: from proteases to maladaptive plasticity. *Frontiers in cellular Neuroscience*. 2019;13:397.
92. Silverman IE, Restrepo L, Mathews GC. Poststroke seizures. *Archives of neurology*. 2002;59(2):195-201.
93. Sarecka-Hujar B, Kopyta I. Poststroke epilepsy: current perspectives on diagnosis and treatment. *Neuropsychiatric disease and treatment*. 2018:95-103.
94. Harris B, Gollo LL, Fulcher BD. Tracking the distance to criticality in systems with unknown noise. *Physical Review X*. 2024;14(3):031021.
95. Herrmann CS, Murray MM, Ionta S, Hutt A, Lefebvre J. Shaping intrinsic neural oscillations with periodic stimulation. *Journal of Neuroscience*. 2016;36(19):5328-5337.
96. Cocchi L, Sale MV, L Gollo L, et al. A hierarchy of timescales explains distinct effects of local inhibition of primary visual cortex and frontal eye fields. *elife*. 2016;5:e15252.
97. Gollo LL, Roberts JA, Cocchi L. Mapping how local perturbations influence systems-level brain dynamics. *Neuroimage*. 2017;160:97-112.
98. Vosskuhl J, Strber D, Herrmann CS. Non-invasive brain stimulation: a paradigm shift in understanding brain oscillations. *Frontiers in human neuroscience*. 2018;12:211.
99. Lakatos P, Gross J, Thut G. A new unifying account of the roles of neuronal entrainment. *Current Biology*. 2019;29(18):R890-R905.
100. Assenza G, Capone F, Di Biase L, et al. Oscillatory activities in neurological disorders of elderly: biomarkers to target for neuromodulation. *Frontiers in Aging Neuroscience*. 2017;9:189.
101. Asl MM, Valizadeh A. Entrainment by transcranial alternating current stimulation: Insights from models of cortical oscillations and dynamical systems theory. *Physics of Life Reviews*. 2025;

Figure legends

Figure 1. One-month post-stroke analysis of intrinsic neural timescales. **A**. fMRI from 15 stroke patients were collected. **B**. Brain parcellation comprising 32 regions of interest (ROIs) organized into 8 functional networks—Default Mode Network (DMN), Sensorimotor Network (SMN), Visual Network (VIS), Salience Network (SAN), Language Network (LN), Frontoparietal Network (FPN), Dorsal Attention Network (DAN), and Cerebellar Network (CE)—was utilized to extract regional BOLD time series. **C**. Intrinsic neural timescales were estimated by calculating the area under the curve in which the autocorrelation function (ACF) is positive. Compared to healthy controls, stroke patients exhibited significantly longer INT both globally, for the whole brain (**D**) and within specific functional networks (**E**). **F**. Hierarchical Intrinsic Neural Timescales are also disrupted after a stroke.

Figure 2. Impact of stroke on intrinsic neural timescales. **A**. Prolonged INT observed in stroke patients persists up to five months post-stroke. **B**. Whole-brain map showing prolonged INT in stroke patients at 1-month post-stroke (PAT1). **C**. At 2 months post-stroke (PAT2), significant differences in INT emerged between patients with good and poor recovery outcomes. **D**. Network-level differences in INT between good and poor outcome groups at PAT2.

Figure 3. Stroke lesions prolong intrinsic neural timescales and alter network dynamics. Stroke shifts the brain dynamics from a slightly subcritical state (blue) toward criticality (red), with the potential to enter a supercritical state. Near a phase transition, cortical network dynamics can be modelled as a branching process, where intrinsic neural timescales peak at the critical point.[15] Stroke-induced shifts toward criticality may eventually drive the system into a supercritical phase, marked by runaway activity that could manifest as seizures. This result is an average of 50 trials.

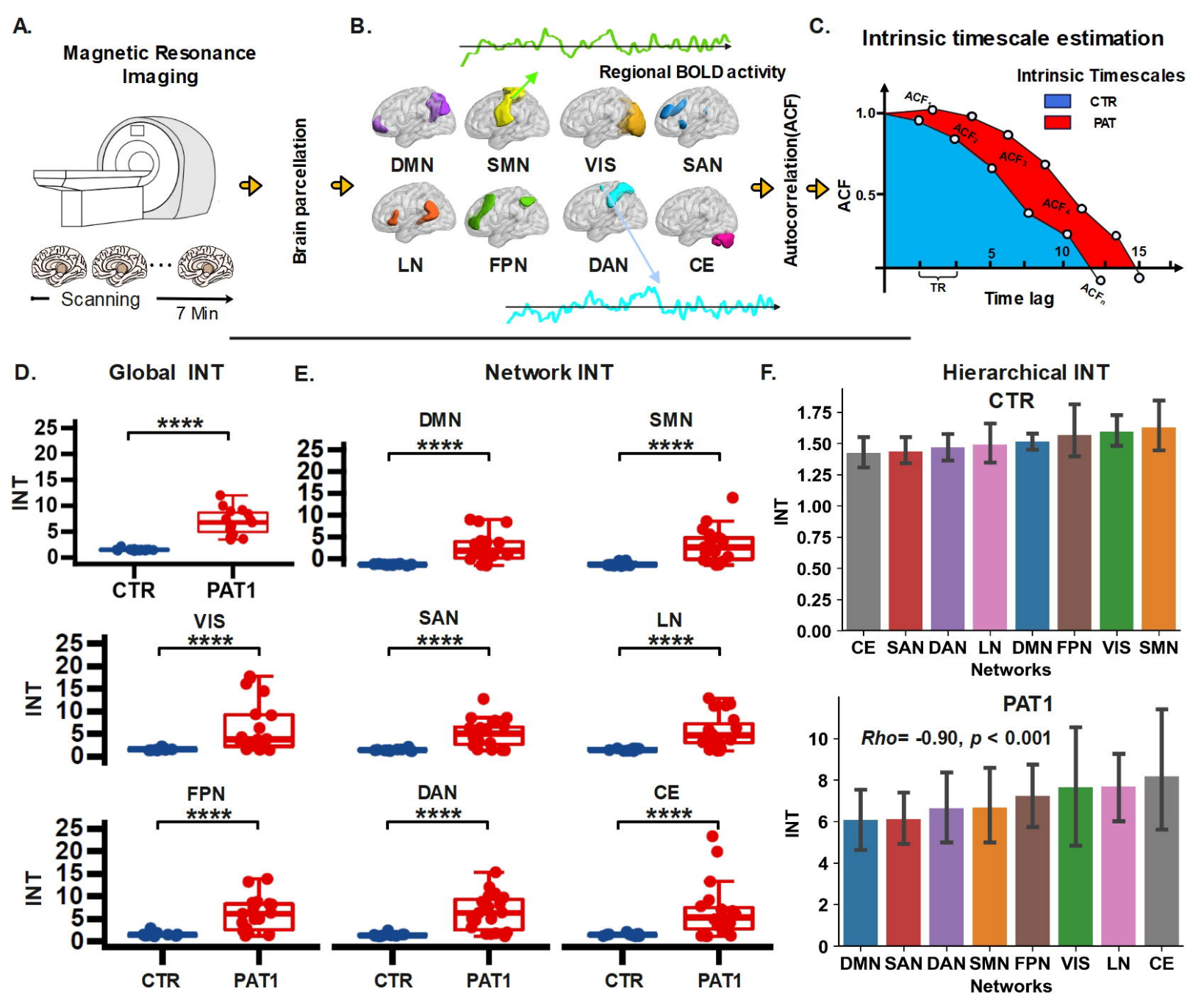
A.
Magnetic Resonance Imaging
Scanning
7 Min
Brain parcellation
B.
Regional BOLD activity
DMN
SMN
VIS
SAN
LN
FPN
DAN
CE
Autocorrelation(ACF)
C.
Intrinsic timescale estimation
Intrinsic Timescales
CTR
PAT
ACF
Time lag
TR
D.
Global INT
INT
CTR
PAT1
E.
Network INT
DMN
SMN
VIS
SAN
LN
FPN
DAN
CE
F.
Hierarchical INT
CTR
PAT1
Rho= -0.90, p < 0.001
Networks

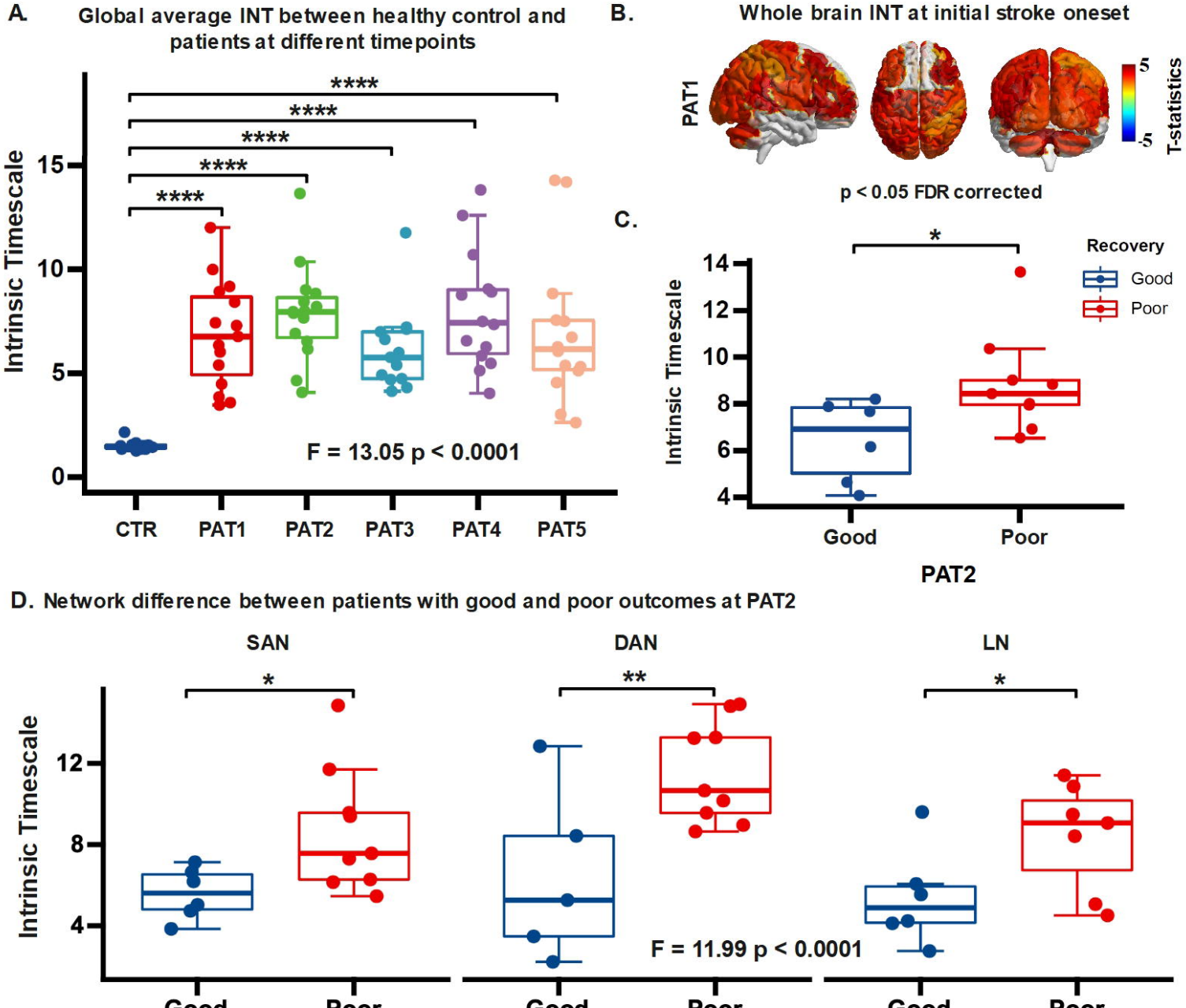
A.
Global average INT between healthy control and patients at different timepoints
Intrinsic Timescale
****
****
****
****
****
F = 13.05 p < 0.0001
CTR
PAT1
PAT2
PAT3
PAT4
PAT5
B.
Whole brain INT at initial stroke oneset
PAT1
T-statistics
p < 0.05 FDR corrected
C.
Recovery
Good
Poor
Intrinsic Timescale
PAT2
D. Network difference between patients with good and poor outcomes at PAT2
SAN
DAN
LN
Intrinsic Timescale
F = 11.99 p < 0.0001
Good
Poor

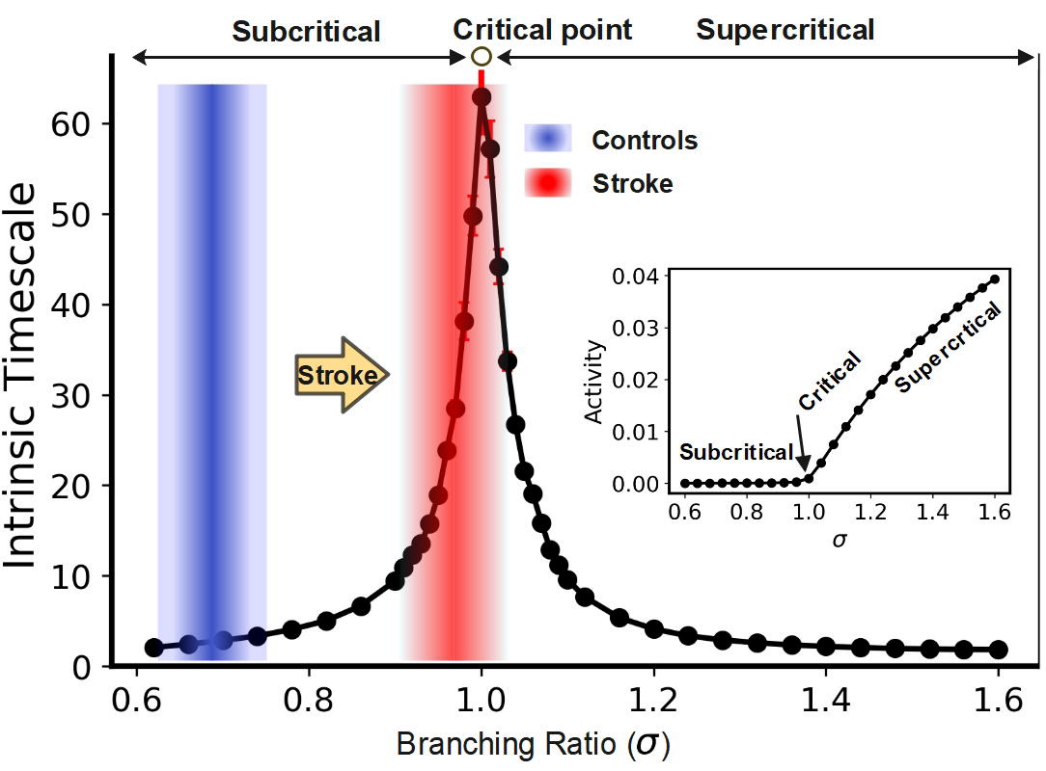
Subcritical
Critical point
Supercritical
Controls
Stroke
Stroke
Intrinsic Timescale
Branching Ratio (σ)
0
10
20
30
40
50
60
0.6
0.8
1.0
1.2
1.4
1.6
Activity
σ
Subcritical
Critical
Supercrtical
0.00
0.01
0.02
0.03
0.04